

## Concealed Magnetic Parent Phase in Iron Oxypnictide Superconductor

High-temperature superconductivity appears by carrier doping to an undoped parent compound; therefore, the physical properties of the parent are strongly related to the superconducting state. We report the discovery of a unique structural transition as well as an antiferromagnetic phase in  $\text{LaFeAsO}_{1-x}\text{H}_x$  ( $x \sim 0.5$ ) even though the electrical and magnetic interactions are generally expected to be weak in the overdoped region. The unprecedented two-dome superconducting phases can be interpreted as a consequence of the carrier doping starting from the original ( $x \sim 0$ ) and advanced ( $x \sim 0.5$ ) parent phases towards the intermediate region.

A new class of high-temperature (high- $T_c$ ) superconductors, iron-based materials, following the cuprates has been widely studied since their discovery in 2008 [1, 2]. In the first obtained iron-based superconductor, tetragonal  $\text{ZrCuSiAs}$ -type  $\text{LaFeAsO}$  [Fig. 1(a)], the superconductivity appears by carrier doping to the undoped parent of the magnetic- and structural-ordered state [3, 4]. An advanced doping method using a hydrogen anion instead of fluorine in  $\text{LaFeAsO}$  surpassed the doping limit of fluorine, and revealed a second superconducting phase (SC2) ( $T_{c,\text{max}} = 36$  K at  $x \sim 0.35$ ), in addition to the first dome (SC1) ( $T_{c,\text{max}} = 26$  K at  $x \sim 0.1$ ) [5]. In order to determine whether a certain hidden phase exists beyond the SC2 region, we performed a multi-probe study using X-ray, neutron, and muon beams in the range  $0.40 \leq x \leq 0.51$ .

X-ray powder diffraction measurements were performed on the beamlines of 8A/8B at KEK-PF. Neutron powder diffractions were measured on Super HRPD and NOVA at J-PARC. The muon spin relaxations were conducted at J-PARC MUSE and PSI.

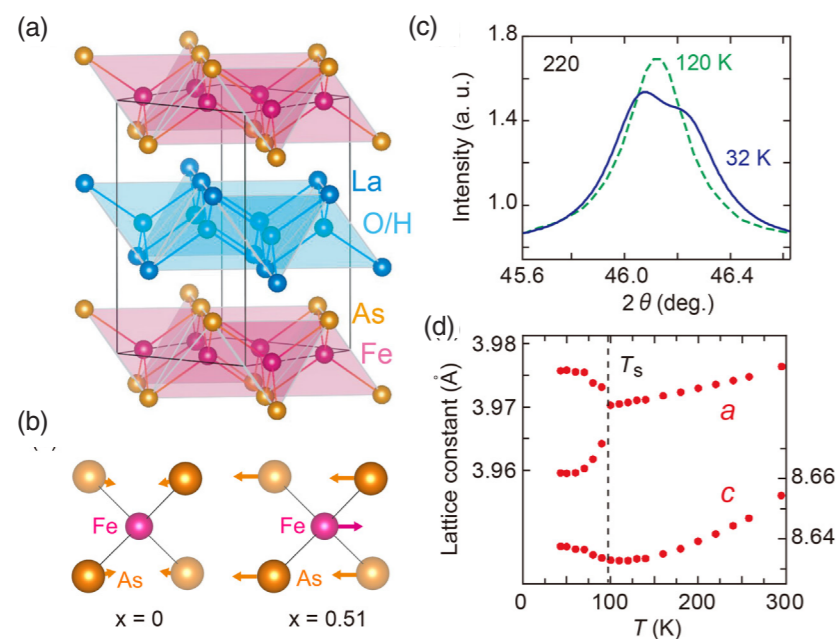


Figure 1: (a) Crystal structure of  $\text{LaFeAsO}$ . (b) Arrows on the  $\text{FeAs}_4$  tetrahedra across the structural transitions represent the displacements of the Fe and As atoms by  $0.07 \text{ \AA}$  ( $0 \text{ \AA}$ ) and  $0.06 \text{ \AA}$  ( $0.01 \text{ \AA}$ ) in  $x = 0.51$  ( $x = 0$ ), respectively. (c) X-ray profile of  $(2, 2, 0)_T$  reflection in  $\text{LaFeAsO}_{0.49}\text{H}_{0.51}$ . (d) Temperature dependence of the lattice constant of  $\text{LaFeAsO}_{0.49}\text{H}_{0.51}$ .

Figure 1(c) shows the X-ray profile of the  $(2, 2, 0)_T$  reflection in the non-superconducting specimen with  $x = 0.51$ . On cooling, the peak of  $(2, 2, 0)_T$  broadened, while no broadening of the  $(0, 0, 6)_T$  and  $(2, 0, 0)_T$  peaks was observed [6]. These experimental findings indicate that the tetragonal to orthorhombic structural transition emerges clearly for  $x = 0.51$ . Figure 1(d) shows the temperature dependence of the lattice parameters for  $x = 0.51$ . The  $a$ -axis length splits in two below the structural transition of  $T_s \sim 95$  K, and the  $c$ -axis shows an upturn at  $T_s$ . Precise X-ray powder-diffraction structural analysis with the RIETAN-FP program [7] using a high-resolution synchrotron radiation source indicates that the  $x = 0.51$  compound crystallizes in an orthorhombic non-centrosymmetric  $Aem2$  structure below  $T_s$  in contrast to the centrosymmetric  $Cmme$  structure for  $x = 0$ . Across the structural transition, only the As atoms move slightly in  $x = 0$ , while the Fe and As atoms move in antiphase in  $x = 0.51$  as shown in the inset of Fig. 1(b).

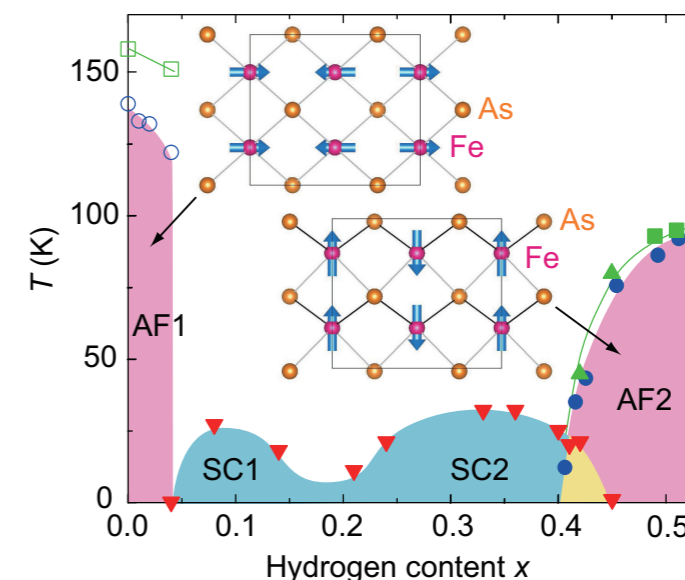


Figure 2: Magnetic, structural and superconducting phase diagram of  $\text{LaFeAsO}_{1-x}\text{H}_x$ . First and second superconducting phases (SC1 and SC2) are thought to be generated by starting from the original and advanced antiferromagnetic phases (AF1 and AF2), respectively. The crystal structures and magnetic Fe spin arrangements of AF1 and AF2 in the Fe-As planes are illustrated [9]. The structural, magnetic, and superconducting transitions are indicated by the green, blue, and red marks, respectively.

In the neutron powder diffraction measurement for  $x = 0.51$ , we observed magnetic peaks below  $T_N = 89$  K with the propagation vector of  $\mathbf{q} = (1/2, 1/2, 0)$ . The result of magnetic structure analysis using the FullProf program [8] reveals an exceptional stripe-type arrangement among the iron-pnictides as shown in the inset of Fig. 2. The estimated magnetic moment  $1.2 \mu_B$  per iron atom is significantly larger than the value of  $0.63 \mu_B$  for  $x = 0$  [6]. In the muon spin relaxation measurements, we observed that the value of  $T_N$  and the magnetic volume fraction decrease in unison with decreasing hydrogen content from  $x = 0.51$ . Moreover, the coexistence state of the antiferromagnetic static order and the superconducting state was found in the range  $0.40 \leq x \leq 0.45$  despite the absence of the coexistence state in the underdoped region [6].

Figure 2 illustrates the phase diagram of  $\text{LaFeAsO}_{1-x}\text{H}_x$  [6]. We consider that a new antiferromagnetic phase with the structural transition next to the superconducting phase can be regarded as the *doped parent phase* by analogy of the undoped antiferromagnetic parent phase with the structural transition. This is unexpected because magnetic and electronic interactions are usually perceived as being weak in the highly carrier-doped region. In the iron-pnictides, the parent compound not only refers to the undoped compound but also more generally indicates a certain critical point of the magnetic and electronic correlations. Moreover, we can definitely state

that the two SC domes are generated by carrier-doping to the left- and right-hand parent compounds towards the intermediate region of the phase diagram.

### REFERENCES

- [1] Y. Kamihara, H. Hirata, M. Hirano, R. Kawamura, H. Yanagi, T. Kamiya and H. Hosono, *J. Am. Chem. Soc.* **128**, 10012 (2006).
- [2] Y. Kamihara, T. Watanabe, M. Hirano and H. Hosono, *J. Am. Chem. Soc.* **130**, 3296 (2008).
- [3] J. Paglione and R.L. Greene, *Nature Phys.* **6**, 645 (2010).
- [4] D.J. Singh and M.-H. Du, *Phys. Rev. Lett.* **100**, 237003 (2008).
- [5] S. Iimura, S. Matsuishi, H. Sato, T. Hanna, Y. Muraba, S.W. Kim, J.E. Kim, M. Takata and H. Hosono, *Nature Commun.* **3**, 943 (2012).
- [6] M. Hiraishi, S. Iimura, K.M. Kojima, J. Yamaura, H. Hiraka, K. Ikeda, P. Miao, Y. Ishikawa, S. Torii, M. Miyazaki, I. Yamauchi, A. Koda, K. Ishii, M. Yoshida, J. Mizuki, R. Kadono, R. Kumai, T. Kamiyama, T. Otomo, Y. Murakami, S. Matsuishi and H. Hosono, *Nature Phys.* **10**, 300 (2014).
- [7] F. Izumi and K. Momma, *Solid State Phenom.* **130**, 15 (2007).
- [8] J. Rodriguez-Carvajal, *Physica B* **192**, 55 (1993).
- [9] K. Momma and F. Izumi, *J. Appl. Crystallogr.*, **44**, 1272 (2011).

### BEAMLINES

BL-8A and BL-8B

J. Yamaura<sup>1</sup>, M. Hiraishi<sup>2</sup>, K. M. Kojima<sup>2</sup>, H. Hiraka<sup>2</sup>, R. Kadono<sup>2</sup>, T. Kamiyama<sup>2</sup>, T. Otomo<sup>2</sup>, R. Kumai<sup>2,3</sup> and Y. Murakami<sup>2,3</sup> (<sup>1</sup>MCES Tokyo Insti. of Tech., <sup>2</sup>KEK-IMSS, <sup>3</sup>KEK-PF)